

Research Article

Porous Maltodextrin-Based Nanoparticles: A Safe Delivery System for Nasal Vaccines

Rodolphe Carpentier^{1,2,3}, Anne Platel^{4,5}, Norhane Salah^{1,2,3}, Fabrice Nessler^{4,5}, and Didier Betbeder^{1,2,3,6}

¹Inserm, LIRIC-UMR 995, F-59 000 Lille, France

²Université de Lille, LIRIC-UMR 995, F-59 045 Lille, France

³CHRU de Lille, LIRIC-UMR 995, F-59 000 Lille, France

⁴Institut Pasteur de Lille, IMPECS-EA4483, 59019 Lille, France

⁵Université de Lille, IMPECS-EA4483, 59045 Lille, France

⁶Université d'Artois, 62800 Liévin, France

Correspondence should be addressed to Rodolphe Carpentier; rodolphe.carpentier@univ-lille.fr

Received 22 August 2018; Revised 18 October 2018; Accepted 4 November 2018; Published 16 December 2018

Academic Editor: Dong Kee Yi

Copyright © 2018 Rodolphe Carpentier et al. This is an open access article distributed under the Creative Commons Attribution License, which permits unrestricted use, distribution, and reproduction in any medium, provided the original work is properly cited.

Vaccination faces limitations, and delivery systems additionally appear to have potential as tools to trigger protective immune responses against diseases. The nanoparticles studied are cationic maltodextrin-based nanoparticles with an anionic phospholipid core (NPL); they are a promising antigen delivery system, and their efficacy as drug vectors against complex diseases such as toxoplasmosis has already been demonstrated. Cationic compounds are generally described as toxic; therefore, it is of interest to evaluate the behavior of these NPL *in vitro* and *in vivo*. Here, we studied the *in vitro* toxicity (cytotoxicity and ROS induction in intestinal and airway epithelial cell lines) and the *in vivo* tolerability and genotoxicity of these nanoparticles administered by the nasal route to a rodent model. *In vitro*, these NPL were not cytotoxic and did not induce any ROS production. *In vivo*, even at very large doses (1000 times the expected human dose), no adverse effect and no genotoxicity were observed in lungs, stomach, colon, or liver. This study shows that these NPL can be safely used.

1. Introduction

Despite pharmaceuticals' proven efficacy in managing several well-described pathologies, many emerging (or indeed established) diseases remain without effective pharmaceutical treatments and/or vaccination strategies. Moreover, with worldwide opinion favoring a reduction in the massive use of antibiotics in both human and veterinary medicine, researchers will need to develop new approaches to both drugs and vaccines. With respect to vaccine efficacy, the use of adjuvants seems to be a prerequisite and two different approaches are envisaged: the use of immunomodulators and/or specific delivery systems [1–3].

Numerous studies have described the use of nanoparticles as an antigen delivery system [4]. Indeed, nanoparticles associate antigens and function as a vector to assist their capture by

the resident immune cells and/or accessory epithelial cells to trigger a protective immune response. Among the wide diversity of nanocarriers, the maltodextrin-based nanoparticles (NPL) are promising for vaccination. NPL are made of reticulated and positively charged (with trimethyl ammonium grafting) maltodextrin, an alpha(1,4)-glucose polymer, filled with an anionic phospholipid core [5]. NPL are porous, and their cationic charge is equally distributed in the material, not merely at the surface; incorporating anionic phospholipids in their core makes NPL zwitterionic [5, 6]. They retain their colloidal stability in biological fluids, behave as a “stealth” nanoparticle [5], and can associate a large quantity (100% w/w) [5] of a wide variety of antigens (e.g., more than 2000 different proteins in a complex mixture of a pathogen lysate) [6, 7].

These NPL nanoparticles have already been successfully developed in our laboratory for toxoplasmosis vaccination

via the nasal route [6]. The NPL-based toxoplasmosis vaccine exhibited a complete protection against the parasitic infection in both chronic and congenital diseases owing to a mixed Th1/Th17 protective immune response [6, 8]. The vaccine formulation consisted of a total extract of the parasite associated with NPL. After intranasal administration, NPL entered the epithelial cells to deliver the antigens and were exocytosed. They were finally swallowed and totally eliminated within 3 days *via* the intestinal tract [9]. Furthermore, biodistribution analyses did not show any evidence of passage into blood or lymph, thus precluding organ accumulation [9].

The nasal route of administration is preferable since the nasal mucosa is the first barrier for many pathogens. Nasal vaccination can induce a systemic and global mucosal immunity, and the nasal cavity is also an easily accessible, immune-competent tissue that enables noninvasive, needle-free vaccine administration [4].

In order to pursue the development of NPL-based vaccines, the toxicity of this nanocarrier must be examined. In this study, we assess the *in vitro* cytotoxicity of the NPL by analyzing the cell's viability and the reactive oxygen species (ROS) production of airway (NCI-H292) and intestinal (Caco2) epithelial cells treated with NPL. The *in vivo* genotoxicity was also investigated using the comet assay in rats treated with more than 1000 times the expected human NPL dose.

2. Methods

2.1. NPL Synthesis and Characterization. NPL were prepared as described previously [6]. Briefly, maltodextrin (Roquette, France) was dissolved in 2 N sodium hydroxide with magnetic stirring at room temperature. They were reticulated and cationized using epichlorohydrin and GTMA (glycidyl trimethyl ammonium chloride, Sigma-Aldrich, France) to obtain hydrogels that were neutralized with acetic acid and sheared using a high-pressure homogenizer. The nanoparticles obtained thus were purified in ultrapure water by tangential flow ultrafiltration using a 750 kDa membrane, then mixed with DPPG (1,2-dipalmitoyl-*sn*-glycero-3-phosphatidylglycerol, Lipoid, France) above the gel-to-liquid phase transition temperature to produce NPL. The size (*Z*-average) and the zeta potential of the NPL were measured in water with the zetasizer nanoZS (Malvern Instruments, France) by dynamic light scattering and by electrophoretic mobility analysis, respectively.

NPL were imaged using a low-voltage (5 kV) transmission electron microscope LVEM5-TEM (DeLong Instruments, Brno, Czech Republic). Samples were prepared by placing 5 μ L (5 mg/mL) of NPL on 300 mesh ultrathin carbon film copper grids (Cu300-HD from Pacific Grid-Tech, San Francisco, USA). After removal of the excess water using a filter paper, the TEM grids were air-dried at room temperature for 10 minutes prior to analysis [6].

2.2. Cell Culture. The NCI-H292 (H292) airway epithelial cells (ATCC CRL-1848) were maintained in DMEM supplemented with 10% (*v/v*) heat-inactivated fetal calf serum (hiFCS), 100 U/mL penicillin, 100 μ g/mL streptomycin,

and 2 mM L-glutamine at 37°C in a humidified, 5% CO₂ atmosphere.

The Caco2 intestinal epithelial cells (ATCC HTB-37) were maintained in DMEM supplemented with 20% (*v/v*) heat-inactivated fetal calf serum (hiFCS), 100 U/mL penicillin, 100 μ g/mL streptomycin, and 2 mM L-glutamine at 37°C in a humidified, 5% CO₂ atmosphere.

2.3. Measurement of Cellular Viability. H292 or Caco2 cells were seeded at a density of 2×10^4 cells in a 96-well plate for 72 h. The culture medium was replaced, and increasing amounts of NPL were added for 3 hours directly to cells, from 0 to 150 μ g/cm². The cellular viability was measured by two methods. Firstly, the mitochondrial activity was assessed by the MTT method using the CellTiter 96 nonradioactive cell proliferation assay kit (Promega, France), an MTT-induced tetrazolium-to-formazan conversion, according to the manufacturer's instructions. After treatment, cells were washed with PBS and 15% (*v/v*) of a dye solution was added and left for 3 hours at 37°C, then stopped. After 1 hour, absorbance was read at 590 nm on a Multiskan GO spectrophotometer (Thermo Scientific, France). The negative control was untreated cells, while 4% (*v/v*) paraformaldehyde (20 min at 37°C) was used as a positive control. In parallel, the cell membrane integrity was determined with the CytoTox 96 nonradioactive cytotoxicity assay kit (Promega, France), an LDH-induced tetrazolium-to-formazan conversion, according to the manufacturer's instructions. The LDH content was determined in the clarified cell supernatants (centrifugation at 100g, 5 minutes at room temperature). The reaction was performed for 30 min at 37°C then stopped, and absorbance were read at 490 nm on a Multiskan GO spectrophotometer. The negative control was the untreated cells while the positive control was established using a treatment with 10% (*v/v*) Triton X-100 in PBS. Both methods were performed on the same cells by multiplexing the procedures.

2.4. Measurement of Cells' ROS Production. Caco2 or H292 cells were seeded at a density of 2×10^4 in a 96-well plate for 72 h. Cells were then washed twice with PBS, and 10 μ M of the fluorescent reactive oxygen species (ROS) probe H2DCFDA (2',7'-dichlorofluorescein diacetate, Sigma-Aldrich, France) in PBS was directly added to cells for 30 minutes at 37°C. Cells were then washed twice with PBS then either treated or not with 150 μ g/cm² of NPL and immediately analyzed on a Fluoroskan Ascent (Thermo Scientific, France; excitation: 485 nm, emission: 527 nm). TBHP (*tert*-butyl hydroperoxide), used at 100 μ M, was used as a positive control (not shown). To compare the kinetics of ROS induction in cells, results for each treatment were normalized over the initial time *t*₀ arbitrarily set to 1: $\text{value}(t)/\text{value}(t_0)$.

2.5. In Vivo Genotoxicity Assessment in Rats. The genotoxic activity of NPL, administered *via* the intranasal route using 2 successive daily treatments at 3 dose levels, was tested using the *in vivo* comet assay in rats on isolated lung, stomach, colon, and liver cells, in compliance with the Organization

for Economic Co-operation and Development (OECD) Guideline 489 [10]. Animal procedures were conducted in agreement with European Directive 2010/63/EU for the protection of animals used for scientific purposes and obtained the regional Ethical Committee on Animal Experimentation (CEEA 75) approval. Male OFA Sprague-Dawley rats (Charles River, France), between 5 and 6 weeks old and weighing approximately 200 g, were used. Animals were placed by random distribution in polypropylene cages housed in a ventilated cupboard. The temperature was $22 \pm 2^\circ\text{C}$, and humidity was $55 \pm 15\%$. Ventilation renewed the air 20 times per hour, and a timer provided light 12 hours a day (8 a.m.–8 p.m.). After acclimatization for five days, animals were divided into 5 groups (5 animals/group). Treatments were performed on nonanesthetized animals. Three groups were treated by intranasal route with NPL at the selected doses of 8, 4, or 2 mg/kg/day ($\times 2$). NPL was suspended in sterile water at concentrations of 2.5, 5, and 10 mg/mL with a volume of administration of 0.8 mL/kg. A control group received sterile water intranasally, and a positive control group was treated orally with MMS (methyl methane sulfonate 100 mg/kg/day ($\times 2$) in physiological water). Animal body weights were recorded before each administration while clinical signs were monitored daily. Animals were anesthetized with isoflurane and sacrificed by exsanguination 2 to 6 hours after the final administration of NPL.

A portion of the lung, stomach, colon, and liver was collected and washed in the cold fresh mincing buffer (10% *v/v* 200 mM EDTA, 80% *v/v* HBSS without phenol red, and 10% *v/v* DMSO, pH 7.5) to remove blood. The tissue portion was minced with a pair of fine scissors to release the cells. Cell suspensions were stored on ice for 15–30 seconds to allow large clumps to settle. The whole cell suspension was harvested, and 2×10^4 viable cells from each suspension were processed for slide preparation. Cells were mixed with low melting point agarose 0.5% *w/v*, kept at 37°C , and transferred onto three independent agarose precoated slides (two layers of normal agarose (1.5% *w/v* and 0.8% *w/v*)). All steps were sheltered from daylight to prevent the occurrence of additional DNA damage. After the top layer of agarose had solidified, slides were immersed for at least 1 hour at $+4^\circ\text{C}$ in the dark in a lysis solution (2.5 M NaCl, 100 mM EDTA, 10 mM Trizma base, pH 10 supplemented with 1% *v/v* Triton X-100 and 10% *v/v* DMSO; pH adjusted to 10 with NaOH) then placed in a fresh electrophoresis solution (1 mM EDTA and 300 mM NaOH, pH > 13) for 20 minutes to allow DNA unwinding and expression of single-strand breaks and alkali-labile sites. Next, electrophoresis was conducted for 20 minutes at 4°C (25 V, 300 mA). Slides were then neutralized for 2×5 minutes in a 0.4 M Tris solution (pH 7.5), and gels were dehydrated by immersion in absolute ethanol for 5 minutes. Slides were air-dried and stored at room temperature. Just prior to scoring, the DNA was stained using propidium iodide (20 $\mu\text{g/mL}$ distilled water, 25 $\mu\text{L/slide}$). After coding slides, 150 randomly selected cells per animal (i.e., 50 cells per slide) were analyzed with a 200x magnification using a fluorescent microscope (Leica Microsystems, Switzerland), equipped with an excitation filter of 515–560 nm and a barrier filter of 590 nm, connected to the

Comet Assay IV Image Analysis System (version 4.11, Perceptive Instruments Ltd., UK). DNA damage was expressed as a percentage of DNA in the tail (% tail intensity) [11, 12]. Statistical analyses were performed with StatView® Software (version 5.0, SAS Institute Inc., USA). The nonparametric Kruskal-Wallis test was used to examine a possible dose-effect relationship. Moreover, the statistical significance of differences in the median values between each group versus control was determined with the nonparametric Mann-Whitney *U* test. Data were considered significantly different when $p < 0.05$.

2.6. Evaluation of the NPL Tolerability. The tolerability of the NPL was studied throughout the experiment. The animals were weighed before the first nasal administration and before sacrifice. The percentage of variation was calculated, and statistical tests (one-way ANOVA with Tukey's post hoc test) were performed to determine the effect of NPL on the weight variation. The behavior of the rats was also observed with particular attention being paid to sneezing, nose bleeds, runny nose, or watery eyes during the 15 minutes following nasal administration; anxiety, pain-related disorders (aggressiveness, lack of movement, hunched posture, piloerection, ear position, eye tightening, and grooming), and death were also recorded until sacrifice.

3. Results

3.1. Characterization of NPL. NPL are porous maltodextrin-based nanoparticles with a lipid core. NPL are spherical nanoparticles as determined by low-voltage TEM under ambient pressure and temperature. This method avoided crushing the low-density NPL due to the freezing or vacuum conditions necessary for other EM analyses and hence preserved the structure of the NPL (Figure 1). The size of NPL was determined by dynamic light scattering, and an average size of 92 nm with a polydispersity index (PDI) of 0.2 was measured, meaning the size of NPL was homogeneous. The zeta potential, indicating the surface charge of the NPL, was determined to be +31 mV (Table 1). These results confirmed that the anionic lipids used were located in the core of these NPL.

3.2. Evaluation of the In Vitro Cytotoxicity of NPL. The cellular viability was studied in two epithelial cellular models representative of the main types of cells that NPL would encounter after nasal administration [9]; it was determined using a nanoparticle concentration range of 0 to 150 $\mu\text{g/cm}^2$ with a combination of MTT and LDH assays. In airway epithelial H292 cells, the viability did not decrease after NPL treatment and a slight increase was even observed (Figure 2(a)). In parallel, the cellular mortality was evaluated and NPL did not induce cell death (Figure 2(b)). In intestinal epithelial Caco2 cells, NPL gave similar results and also showed a lack of any cytotoxicity (Figures 2(c) and 2(d)).

3.3. Evaluation of the In Vitro ROS Production. The production of reactive oxygen species (ROS) was then addressed in the two epithelial cell lines. In airway epithelial H292 cells, a progressive increase of the basal ROS production was

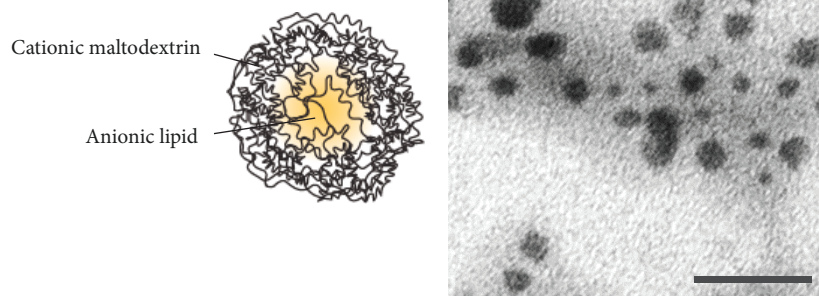


FIGURE 1: Schematic view of the NPL. (a) NPL are porous cationic maltodextrin-based nanoparticles with an anionic lipid core. (b) Representative microphotograph using a low-voltage transmission electronic microscope. NPL appear in black while residual aqueous diluent is in grey. The scale bar is 100 nm.

TABLE 1: Characterization of the NPL. The Z-average size (nm) and the polydispersity index (PDI) of NPL were determined by dynamic light scattering while the zeta potential was by electrophoretic mobility. NPL were measured in triplicate, and values represent the mean \pm SD of a representative synthesis.

	Size (Z-average, nm) \pm SD	PDI \pm SD	Zeta potential (mV) \pm SD
NPL	92.80 \pm 2.82	0.23 \pm 0.01	31.07 \pm 0.67

observed, attributable to the basal oxidative metabolism of the cells. After five hours, NPL neither increased nor decreased ROS production (Figure 3(a)) which means that NPL did not induce the production of free radicals. The same results were observed in intestinal epithelial Caco2 cells (Figure 3(b)).

3.4. In Vivo Tolerability of NPL. The tolerability of NPL administered by the intranasal route was assessed from the first administration to sacrifice. The weight of the rats increased in all groups, whether NPL were administered by 2 to 8 mg/kg/day ($\times 2$) or not. No immediate postadministration reaction was observed (sneezing, nose bleeding, runny nose, or tear dropping; Table 2), and NPL did not provoke any visible signs of pain or anxiety throughout the experiment.

3.5. In Vivo Genotoxicity of NPL. To validate the *in vitro* safety of NPL, the genotoxic potential of NPL was investigated by the *in vivo* comet assay in isolated cells from the rats' lung, stomach, colon, and liver. Rats were nasally administered on two consecutive days with 0 to 8 mg/kg of NPL, followed by one expression time of 2 to 6 hours after the last treatment according to the OECD test guideline 489 [10]. The measured genotoxicity, expressed as the percentage of tail intensity, is given in Figure 4. Very low levels of DNA migration were observed in all the selected organs, with values ranging from 1.76 to 7.42% (vs. 1.15% for the negative control) in the lung (Figure 4(a)), from 11.85 to 21.39% (vs. 13.62% for the negative control) in the stomach (Figure 4(b)), from 22.21% to 23.48% (vs. 18.28% for the negative control) in the colon (Figure 4(c)), and from

0.41% to 0.46% (vs. 0.49% for the negative control) in the liver (Figure 4(d)). No statistically significant difference against the negative control was observed, whatever the tested doses or the organ studied. In the MMS-treated group, used as a positive control, the DNA migration percentage ranged from 54% to 61%. Therefore, NPL administered by the nasal route do not provoke genotoxic activity, irrespective of the dose administered or the organ studied.

4. Discussion

NPL are porous nanoparticles composed of reticulated cationic maltodextrin and filled with anionic phospholipids [5]. They have already shown great potential for mucosal vaccine applications, especially by the nasal route [4, 6, 8]. NPL can be loaded with large amounts of proteins or antigens [5, 13] and act as an efficient delivery system. Upon nasal administration, NPL enter the cells by endocytosis and return to the lumen through exocytosis [13], without crossing the first epithelial cell layer [9]. During this cellular journey, NPL deliver their cargo of antigens, the first step in triggering an immune response.

Despite all the advantages of using NPL for vaccine application (stability, needle-free nasal route of administration, ease of antigen formulation with the nanoparticles, and efficiency of the immune response), no data have yet been published regarding their toxicity. For the first time, here, we clearly demonstrate that these nanoparticles are not toxic, thereby strengthening the case for their use in mucosal vaccines.

At the cellular level, the mechanisms of the nanomaterials' toxicity include (i) the oxidation of biological components *via* the formation of ROS, RNS, and free radicals, (ii) the perforation of the cell membrane, (iii) damage to the cytoskeleton, (iv) DNA damage, (v) mitochondrial damage, or (vi) interference with the formation of lysosomes [14]. In this study, we did not observe any *in vitro* cytotoxicity. Instead, a slight increase in the cell viability was observed (Figures 2(a) and 2(c)). Contrary to other positively charged nanoparticles [15], the NPL did not induce any ROS free radicals in epithelial cell lines, underlining the absence of cytotoxicity (Figure 3). Moreover, we did not show any cell

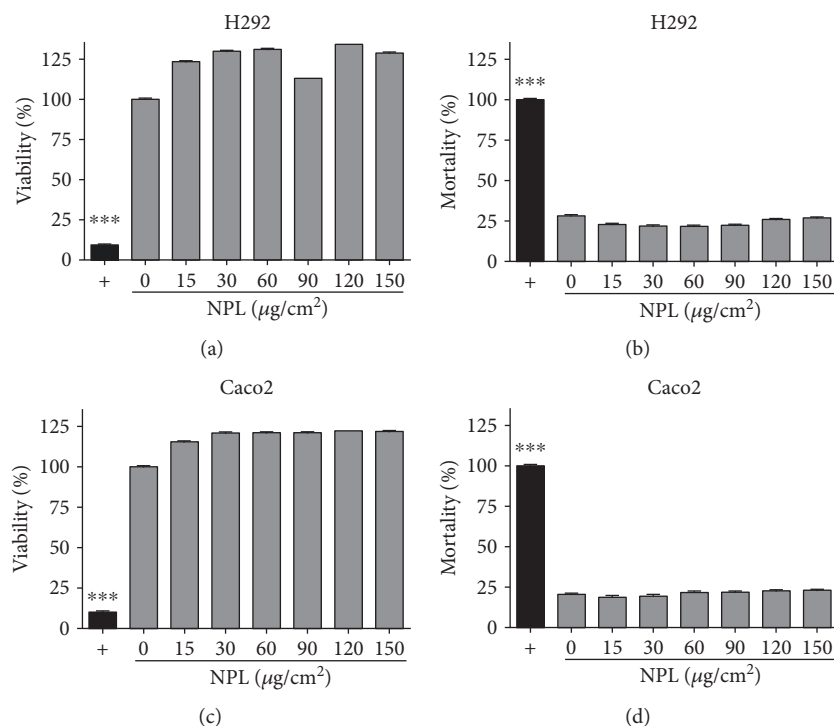


FIGURE 2: Evaluation of the cytotoxicity of NPL. The mitochondrial activity (referred to as viability (a, c)) and the membrane integrity (referred to as mortality (b, d)) in H292 airway (a, b) and Caco2 intestinal (c, d) epithelial cells were, respectively, determined by the MTT and the LDH assays. Cells were seeded in a 96-well plate and treated with NPL from 0 (negative control) to $150 \mu\text{g}/\text{cm}^2$. The cells were analyzed with the MTT assay while the supernatants of treated cells were collected for the LDH assay. Positive controls (+) correspond to cells treated with either 4% (v/v) paraformaldehyde to induce the minimal MTT value or with 10% (v/v) Triton X-100 to induce the maximal LDH release, and 100% was set over the negative control. Data represent the mean \pm SD of the percentage of viability or mortality. No significant difference was observed between 0 (untreated cells) and the NPL-treated cells.

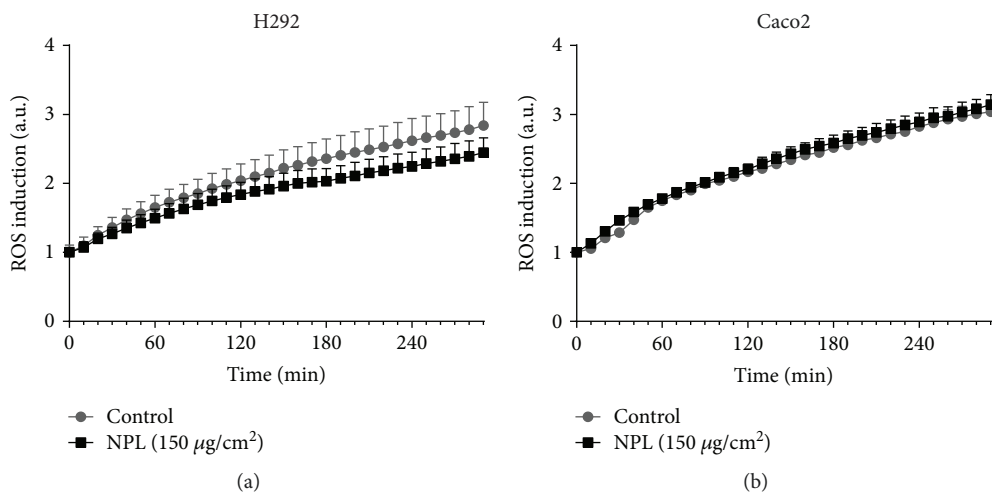


FIGURE 3: Induction of reactive oxygen species (ROS) by NPL. H292 airway (a) or Caco2 intestinal (b) epithelial cells were seeded in a 96-well plate and probed with H2DCF-DA to detect ROS. Cells were then treated with vehicle (control) or with $150 \mu\text{g}/\text{cm}^2$ of NPL and immediately recorded for ROS induction using the Fluoroskan Ascent (Thermo Scientific, France) at the wavelengths (excitation/emission) 488 nm/527 nm. Data represent the mean fluorescence intensity \pm SD normalized over the initial time t_0 arbitrarily set to 1. No significant difference was observed over the negative control. Not shown: $p < 0.0001$ positive control ($100 \mu\text{M}$ TBHP) vs NPL treatment.

membrane alteration (LDH assay), mitochondrial activity disturbance (MTT assay), nor any DNA damage (including oxidative DNA damage) thus supporting our observed

absence of ROS induction. These complementary results provide strong evidence in favor of the safety of these nanoparticles.

TABLE 2: *In vivo* tolerability of the NPL. The mean weight variation (%) of the rats from the control (0) or the NPL-treated groups (2, 4, and 8 mg/kg/day ($\times 2$)) between nasal administration and sacrifice is reported. The expected immediate adverse effects, including sneezing, nose bleeding, runny nose, and watery eyes, were observed and recorded for 15 minutes after nasal administration. The anxiety- and pain-related behaviors and endpoints including aggressiveness, lack of movement, hunched posture, piloerection, ear position, eye tightening, or grooming were observed throughout the *in vivo* genotoxicity assessment. Finally, the percentage of mortality was also recorded.

NPL ((mg/kg/day) $\times 2$)	0	2	4	8
Mean weight variation (%) (% min : % max)	+2.20 (0 : 4.12)	+2.68 (0.92 : 5.41)	+2.02 (0 : 4.71)	+2.36 (−1.95 : 6.19)
Sneezing	No	No	No	No
Nose bleeding	No	No	No	No
Runny nose	No	No	No	No
Watery eyes	No	No	No	No
Itching	No	No	No	No
Anxious behavior	No	No	No	No
Death (%)	0	0	0	0

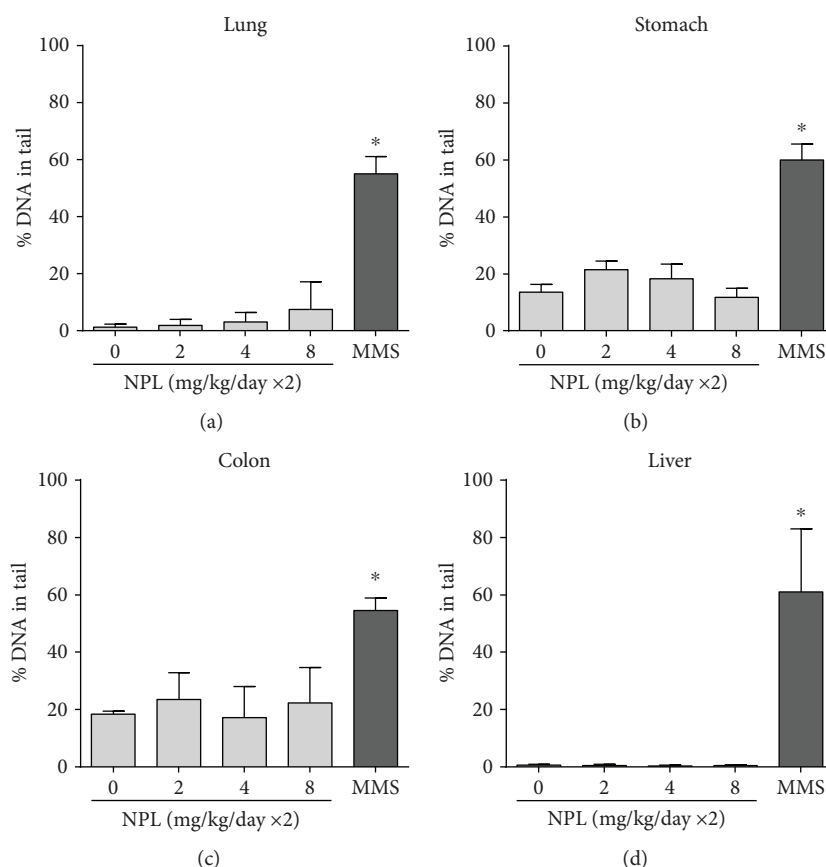


FIGURE 4: *In vivo* genotoxicity of NPL. DNA damage was assessed by the *in vivo* comet assay in the lung (a), stomach (b), colon (c), and liver (d), after 2 consecutive daily intranasal administrations of NPL in rats. For each group, results shown are means of medians of % tail intensity \pm SD for 5 animals. MMS was used as positive control ((100 mg/kg/day) $\times 2$). * $p < 0.05$ positive control vs. all NPL treatments.

The second aim of our study was to investigate the *in vivo* genotoxicity and immediate adverse effects of NPL by using the multiple-organ comet assay in rats. We administered large doses of NPL *via* the nasal route and demonstrated that NPL are not genotoxic *in vivo* (Figure 4), consolidating our *in vitro* observations [16]. Moreover, no adverse

effects were observed in the animals throughout the experiment (Table 2). We also performed a modified comet assay using the human oxoguanine glycosylase hOGG1 [17, 18] in order to determine the oxidative-dependent DNA damage. After NPL treatment, the hOGG1+-modified comet assay did not show any oxidative-dependent DNA

damage (data not shown). This is consistent with the absence of ROS induction (Figure 3) and of genotoxicity without hOGG1 (Figure 4).

At the organism level, the toxicity of a nanomaterial could be due to an accumulation in a specific cell type, tissue, organ, or compartment (e.g., bloodstream) and could lead to the synthesis of inflammatory mediators or complement activation [14]. The NPL were designed to be administered by the mucosal route, preferentially the nasal route. We previously demonstrated that NPL do not cross the nasal epithelium and are totally eliminated *via* the gastrointestinal tract [9]. We have also shown that NPL enter cells by endocytosis and are subsequently completely exocytosed [9, 19] with no intracellular accumulation. This explains the absence of genotoxicity reported in the lung, stomach, or colon (Figures 4(a)–4(c)) and precludes a passage into the bloodstream. Consequently, toxicity at the organism level *via* organ accumulation, opsonization, hemolysis, or extended blood circulation times should not occur. This would seem to be confirmed by both the absence of any genotoxicity in the liver (Figure 4(d)) and the absence of outward clinical signs following administration (Table 2).

Furthermore, we have previously shown that NPL (referred to elsewhere as $_{70}\text{DGNP}^+$) did not activate the complement making them “stealth” regarding the immune system [5]. A local nasal inflammation is possible, but we did not observe any physiological signs postadministration in the current study and concluded that NPL are well tolerated (Table 2). Naturally, these observations do not preclude a study of any potential local inflammation at the cellular and molecular levels.

To ensure the safety of NPL, an excessive dose of nanoparticles was used in our study. The expected human dose has been estimated at $<600\text{ }\mu\text{g}$ by the nasal route of administration (unpublished data). The surface area of the nasal cavities is about 150 cm^2 but could be extent to 100 m^2 if the epithelial microvilli are taken into account [20, 21]. In this study, $150\text{ }\mu\text{g}/\text{cm}^2$ of NPL was used *in vitro* (Figures 2 and 3). Thus, the reported NPL dose in human nasal cavities would range from 22.5 mg ($150\text{ }\mu\text{g}/\text{cm}^2 \times 150\text{ cm}^2$) to 150 g ($150\text{ }\mu\text{g}/\text{cm}^2 \times 100\text{ m}^2$), which means that the *in vitro* doses studied here represent up to 250,000 times the expected human dose. Concerning the *in vivo* experiments, rats received a maximum dose of 8 mg/kg body weight. Considering a person of 75 kg treated with $600\text{ }\mu\text{g}$ of nanoparticles (the expected human dose), the calculated human dose is only $8\text{ }\mu\text{g/kg}$ (1000 times less than the amount tested for determining the *in vivo* genotoxicity).

Other cationic nanoparticles have already been assessed for toxicity, and a comparison of nanoparticles with different surface charges showed that positively charged nanoparticles are more toxic than negatively charged or neutral nanoparticles [22–24]. Cationic nanoparticles can be obtained by coating nanoparticles with a cationizing agent (labile interaction), by chemical grafting of a cationizing agent (stable link) or by using a positively charged material to synthesize the nanoparticles. The coating of nanoparticles with a cationizing agent such as chitosan, cetyltrimethylammonium, or polyethylenimine usually leads to toxicity, even if the nanoparticle material

itself is safe (e.g., the PLGA polymer) [18], probably owing to a leakage of the toxic compound during the decomposition of the nanomaterials [25]. Instead of a surface coating, preparation of positive nanoparticles by the chemical grafting of cationizing agents could also lead to toxicity [23]. Here, we tested cationic nanoparticles obtained by the chemical grafting of a cationizing agent at an early step in their synthesis, before the production of the nanomaterial (top-down approach) [5], and have clearly demonstrated that these cationic NPL are nontoxic. Compared to other nanoparticles, either cationic or anionic, we have demonstrated that NPL rapidly and efficiently entered cells by endocytosis [9, 13, 26]. However, we did not observe any cytotoxicity of NPL in this study. Indeed, NPL have been shown not to accumulate in cells [9], thereby limiting any possibility for toxic effects. This suggests that the production method used to render the nanoparticles cationic is a key factor in avoiding cellular toxicity and must be taken into account in further nanomedicine development.

To conclude, this study performed on rats clearly demonstrates that NPL did not induce ROS, did not modulate cellular viability, and did not cause oxidative or nonoxidative DNA damage even at very high doses. Further studies of a possible local inflammatory reaction after the nasal administration of NPL should be performed. Taken together, this study supports the safety of the NPL used as a delivery system for nasal vaccines.

Data Availability

The authors declare that the data supporting the findings of this study are available within the article and available from the corresponding author upon reasonable request.

Conflicts of Interest

The authors declare no conflict of interest.

Authors' Contributions

Carpentier R. and Platel A. contributed equally to this work.

Acknowledgments

The authors would like to thank Dr. Michael Howsam for critically reading the manuscript and Mrs. Hafssa Jaddi, Mr. Smail Talahari, and Mr. Gonzague Dourdin for their technical assistance. This work did not receive specific funding and was performed with the support of the University of Lille, the INSERM, the CHU Lille, the Pasteur Institute of Lille, and the University of Artois.

References

- [1] E. J. Ryan, L. M. Daly, and K. H. G. Mills, “Immunomodulators and delivery systems for vaccination by mucosal routes,” *Trends in Biotechnology*, vol. 19, no. 8, pp. 293–304, 2001.
- [2] T. Mohan, P. Verma, and D. N. Rao, “Novel adjuvants & delivery vehicles for vaccines development: a road ahead,” *The Indian Journal of Medical Research*, vol. 138, no. 5, pp. 779–795, 2013.

- [3] A. S. McKee and P. Marrack, "Old and new adjuvants," *Current Opinion in Immunology*, vol. 47, pp. 44–51, 2017.
- [4] B. Bernocchi, R. Carpentier, and D. Betbeder, "Nasal nanovaccines," *International Journal of Pharmaceutics*, vol. 530, no. 1–2, pp. 128–138, 2017.
- [5] A. Paillard, C. Passirani, P. Saulnier et al., "Positively-charged, porous, polysaccharide nanoparticles loaded with anionic molecules behave as 'stealth' cationic nanocarriers," *Pharmaceutical Research*, vol. 27, no. 1, pp. 126–133, 2010.
- [6] I. Dimier-Poisson, R. Carpentier, T. T. L. N'Guyen, F. Dahmani, C. Ducournau, and D. Betbeder, "Porous nanoparticles as delivery system of complex antigens for an effective vaccine against acute and chronic *Toxoplasma gondii* infection," *Biomaterials*, vol. 50, pp. 164–175, 2015.
- [7] D. Xia, S. J. Sanderson, A. R. Jones et al., "The proteome of *Toxoplasma gondii*: integration with the genome provides novel insights into gene expression and annotation," *Genome Biology*, vol. 9, no. 7, p. R116, 2008.
- [8] C. Ducournau, T. T. L. Nguyen, R. Carpentier et al., "Synthetic parasites: a successful mucosal nanoparticle vaccine against *Toxoplasma* congenital infection in mice," *Future Microbiology*, vol. 12, no. 5, pp. 393–405, 2017.
- [9] B. Bernocchi, R. Carpentier, I. Lantier, C. Ducournau, I. Dimier-Poisson, and D. Betbeder, "Mechanisms allowing protein delivery in nasal mucosa using NPL nanoparticles," *Journal of Controlled Release*, vol. 232, pp. 42–50, 2016.
- [10] OECD, *Test No. in 489: In Vivo Mammalian Alkaline Comet Assay, OECD Guidelines for Testing of Chemicals, Section 4*, OECD Publishing, Paris, 2014.
- [11] D. P. Lovell and T. Omori, "Statistical issues in the use of the comet assay," *Mutagenesis*, vol. 23, no. 3, pp. 171–182, 2008.
- [12] B. Burlinson, R. R. Tice, G. Speit et al., "Fourth International Workgroup on Genotoxicity testing: results of the in vivo Comet assay workgroup," *Mutation Research/Genetic Toxicology and Environmental Mutagenesis*, vol. 627, no. 1, pp. 31–35, 2007.
- [13] C. Dombu, R. Carpentier, and D. Betbeder, "Influence of surface charge and inner composition of nanoparticles on intracellular delivery of proteins in airway epithelial cells," *Biomaterials*, vol. 33, no. 35, pp. 9117–9126, 2012.
- [14] A. Sukhanova, S. Bozrova, P. Sokolov, M. Berestovoy, A. Karaulov, and I. Nabiev, "Dependence of nanoparticle toxicity on their physical and chemical properties," *Nanoscale Research Letters*, vol. 13, no. 1, p. 44, 2018.
- [15] P. P. Fu, Q. Xia, H. M. Hwang, P. C. Ray, and H. Yu, "Mechanisms of nanotoxicity: generation of reactive oxygen species," *Journal of Food and Drug Analysis*, vol. 22, no. 1, pp. 64–75, 2014.
- [16] M. Merhi, C. Y. Dombu, A. Brient et al., "Study of serum interaction with a cationic nanoparticle: implications for in vitro endocytosis, cytotoxicity and genotoxicity," *International Journal of Pharmaceutics*, vol. 423, no. 1, pp. 37–44, 2012.
- [17] R. Carpentier, A. Platel, H. Maiz-Gregores, F. Nessler, and D. Betbeder, "Vectorization by nanoparticles decreases the overall toxicity of airborne pollutants," *PLoS One*, vol. 12, no. 8, article e0183243, 2017.
- [18] A. Platel, R. Carpentier, E. Becart, G. Mordacq, D. Betbeder, and F. Nessler, "Influence of the surface charge of PLGA nanoparticles on their in vitro genotoxicity, cytotoxicity, ROS production and endocytosis," *Journal of Applied Toxicology*, vol. 36, no. 3, pp. 434–444, 2016.
- [19] C. Y. Dombu, M. Kroubi, R. Zibouche, R. Matran, and D. Betbeder, "Characterization of endocytosis and exocytosis of cationic nanoparticles in airway epithelium cells," *Nanotechnology*, vol. 21, no. 35, article 355102, 2010.
- [20] S. Gizurason, "Anatomical and histological factors affecting intranasal drug and vaccine delivery," *Current Drug Delivery*, vol. 9, no. 6, pp. 566–582, 2012.
- [21] Y. Liu, M. R. Johnson, E. A. Matida, S. Kherani, and J. Marsan, "Creation of a standardized geometry of the human nasal cavity," *Journal of Applied Physiology*, vol. 106, no. 3, pp. 784–795, 2009.
- [22] E. Frohlich, "The role of surface charge in cellular uptake and cytotoxicity of medical nanoparticles," *International Journal of Nanomedicine*, vol. 7, pp. 5577–5591, 2012.
- [23] C. M. Goodman, C. D. McCusker, T. Yilmaz, and V. M. Rotello, "Toxicity of gold nanoparticles functionalized with cationic and anionic side chains," *Bioconjugate Chemistry*, vol. 15, no. 4, pp. 897–900, 2004.
- [24] W. K. Oh, S. Kim, M. Choi et al., "Cellular uptake, cytotoxicity, and innate immune response of silica-titania hollow nanoparticles based on size and surface functionality," *ACS Nano*, vol. 4, no. 9, pp. 5301–5313, 2010.
- [25] B. Pelaz, G. Charron, C. Pfeiffer et al., "Interfacing engineered nanoparticles with biological systems: anticipating adverse nano-bio interactions," *Small*, vol. 9, no. 9–10, pp. 1573–1584, 2013.
- [26] M. Q. Le, R. Carpentier, I. Lantier, C. Ducournau, I. Dimier-Poisson, and D. Betbeder, "Residence time and uptake of porous and cationic maltodextrin-based nanoparticles in the nasal mucosa: comparison with anionic and cationic nanoparticles," *International Journal of Pharmaceutics*, vol. 550, no. 1–2, pp. 316–324, 2018.

